Journal of Invertebrate Pathology 214 (2026) 108458

Contents lists available at ScienceDirect

Journal of Invertebrate Pathology

journal homepage: www.elsevier.com/locate/jip

Pathogen diversity of the non-native narrow-clawed crayfish (*Pontastacus leptodactylus*) in a UK water body☆

Matthew Harwood [a,b,*], Josie South [a,b], Alison M. Dunn [a,b], Paul D. Stebbing [c], Amy Burgess [d,e], Jamie Bojko [d,e,**]

[a] Water@Leeds, University of Leeds, Leeds LS2 9JT, UK
[b] School of Biology, Faculty of Biological Sciences, University of Leeds, Leeds LS2 9JT, UK
[c] APEM Limited, International House, International Business Park, Southampton SO18 2RZ, UK
[d] School of Health and Life Sciences, Teesside University, Middlesbrough TS1 3BX, UK
[e] National Horizons Centre, Teesside University, Darlington DL1 1HG, UK

ARTICLE INFO

Keywords:
Biological invasions
Histopathology
Virology
Freshwater ecology
Crustacea

ABSTRACT

Biological invasions are intrinsically linked to introducing associated symbiotic organisms, some of which can be parasitic or pathogenic. The pathogenic risk of an 'invasive parasite' (aka. exotic pathogen) stems from its potential to infect native hosts and induce behavioural change or mortality, with the pathogen potentially presenting a greater risk than the host. Conversely, parasites translocated by invasive hosts may also reduce the impact of their host, indirectly curbing the hosts impact on the invaded ecosystem. In this study, we develop a pathogen profile for the narrow-clawed crayfish, *Pontastacus leptodactylus*. This is a non-native species in the United Kingdom, and poses a possible risk as a sink for invasive parasites. We use histopathology, metagenomics and metratranscriptomics to outline the symbiotic diversity harboured by a *P. leptodactylus* population from West Yorkshire, England.

We discovered several protozoan and bacterial species that appear to be putatively commensal with this invader, as well as several RNA viruses (*Hepelivirales*; *Picornavirales*; *Nodaviridae*, and others) that may be more pathogenic in nature. Microsporidia and *Nudiviridae* were absent in our population sample set, as were all metazoan obligate parasites, such as trematodes and acanthocephalans. Using the novel genomic and pathological data available to us, we have explored the evolutionary history of each symbiotic species and provided an initial assessment on the putative risk to native species.

1. Introduction

Invasive Non-Native Species (INNS) pose a significant risk to native wildlife, cultured species, and human health, due to their capacity to carry and transmit exotic symbionts, such as parasites and pathogens (also termed, "invasive parasites"; Dunn, 2009; Dunn et al., 2023; Dunn and Hatcher, 2015). These invasive parasites have been shown to affect invasion systems in diverse ways: they can hinder an invader by eliciting population control through behavioural modification, or a reduction in survival (Bojko et al. 2019); or they can may go on to infect native or economically important species (Wood et al. 2023), causing population declines (Svoboda et al. 2017) or other wildlife health impacts (Hatcher et al 2019). Most notably from freshwater environments, *Aphanomyces astaci* (causative agent of crayfish plague) can result in mass white clawed crayfish (*Austropotamobius pallipes*) mortalities, and originates from the invasive asymptomatic host, the signal crayfish (*Pacifastacus leniusculus*; Svoboda et al. 2017).

Outside of the well-studied crayfish plague pathogen, crayfish invasions are also commonly associated with co-invasive symbionts within the groups: Microsporidia (Bojko et al., 2020; Stratton and DiStefano, 2021; Stratton et al. 2022a,b; Stratton et al. 2023a,b; Stratton et al. 2024a); *Nudiviridae* (Stratton et al. 2024b; Petersen et al. 2024); *Psorospermium* sp. (Anaya, 2021; Longshaw et al., 2012); Branchiobdella (Rosewarne et al., 2012); and trematodes (Reisinger et al. 2015). Native

☆ This article is part of a special issue entitled: 'Invertebrate Parasites in Bioinvasions' published in Journal of Invertebrate Pathology.

* Corresponding author at: Water@Leeds, University of Leeds, Leeds LS2 9JT, UK.
** Corresponding author at: School of Health and Life Sciences, Teesside University, Middlesbrough TS1 3BX, UK.
E-mail addresses: bsmhar@leeds.ac.uk (M. Harwood), J.Bojko@tees.ac.uk (J. Bojko).

https://doi.org/10.1016/j.jip.2025.108458
Received 15 April 2025; Received in revised form 19 August 2025; Accepted 15 September 2025
Available online 16 September 2025

crayfish can also harbour mortality-driving groups, such as bunyaviruses, which may play a role in biological invasions (brown spot disease; Grandjean et al. 2019). For example, the *P. leniusculus* invasion of the UK has been linked closely with the spread of *A. astaci*, but also the presence of a 'bacilliform virus', *Psorospermium* sp., branchiobdellids, and the likelihood of acquiring native microsporidian species such as *Astathelohania contejeani* (Dunn et al., 2009; Anderson et al. 2021). Studies such as Anderson et al. (2021) provide geographical detail on symbiont dispersal through invasive/native networks that help to define possible emerging disease risk in wildlife.

Of recent concern to the UK is the narrow-clawed crayfish (*Pontastacus leptodactylus*) and the pathogens that it may harbour. Narrow-clawed crayfish have been broadly introduced across Europe for aquaculture. They are considered data deficient in terms of ecological impact. However, species range is predicted to shift following climate niche changes expected acr oss Europe making them a cause for concern in the future (Hodson et al. 2024). Although *P. leptodactylus* are distributed across England (Peay et al. 2010), we do not know what pathogens may have been co-introduced, or whether they have acquired pathogens in the new range.

Bojko et al. (2021) identified 23 symbionts associated with *P. leptodactylus* from their native and invasive ranges from literature published up to 2017, and since this review a further four have been noted. These include: viruses (*Nimaviridae* and a nudivirus detected through transcriptomic data: 'Astacus leptodactylus nudivirus', which should be putatively termed: 'Pontastacus leptodactylus nudivirus' (AlNV to PlNV; Petersen et al. 2024) due to the recent taxonomic change); bacteria (*Listeria monocytogenes, Aeromonas hydrophila, Shewanella putrefaciens* (Kuzucu and y Özcan, 2025); Microsporidia (*A. contejeani*); Fungi (*Saprolegnia parasitica, Acremonium* sp., *Fusarium solani* (Salighehzadeh et al. 2019), and *Fusarium avenaceum* (Taştan and Akhan, 2021); Protozoa (*Psorospermium haeckeli*, *Branchiobdella* spp., *Chilodonella* spp., *Cothurnia sieboldii*, *Epistylis* spp., *Histricosoma chappuisi*, *Opercularia articulata*, *Podophrya fixa*, *Pyxicola annulata*, *Tetrahymena pyriformis*, *Vorticella similis*, *Zoothamnium intermedium*, and *A. astaci*); and Trematoda (*Astacotrema tuberculatum*).

A combination of technologies can be used to develop pathological surveys of invasive populations, increasing our understanding of pathogen risk by building a baseline pathological view of invasive populations (Foster et al. 2021; Bojko et al. 2023). Such technologies can include classical pathological techniques, such as histology and electron microscopy, and also encompassing more recent techniques, such as metagenomics and metatranscriptomics, which can provide detailed sequence data from an array of pathogens.

The aim of this study is to use histology, metagenomics and metatranscriptomics, to screen narrow-clawed crayfish for symbionts, to better understand the potential for control, and to determine whether they harbour pathogens that may pose a risk to native species.

2. Methods

2.1. Specimen collection and husbandry

Narrow-clawed crayfish (n = 20), *P. leptodactylus*, were collected from Boshaw Whams Reservoir, Holmfirth, West Yorkshire, UK (Lat 53°32′52″N, Long 001°46′23″W) between October 2022 and December 2022. *P. leptodactylus* were first detected around 2014 and local anglers started to report them as a nuisance in 2019 (pers. comm Huddersfield Angling Club). Crayfish were collected under a Natural England trapping license using collapsible fladen crayfish traps (570 mm x 290 mm, 25 mm mesh size) deployed overnight at the reservoir and retrieved after 18 h. All crayfish were transported to the University of Leeds, West Yorkshire and housed in sex segregated holding tanks. The animals were anaesthetised before dissection by being placed in a −20 °C freezer for 10 min, following the methods described by Bojko et al. (2022).

2.2. Histological preparation

Twenty *P. leptodactylus* were prepared for histological analysis, where the muscle, nerve, gill, gonad, heart, gut, hepatopancreas, and antennal gland were biopsied and placed into a single labelled cassette, per crayfish. The tissues were fixed in Davidson's freshwater fixative, and then moved into 70 % ethanol after 24 h. Tissue processing included 90 % and 100 % ethanol infiltration, prior to 2 baths of xylene-substitute, and finally paraffin wax. The tissues were solidified into a block of paraffin wax including the labelled cassette. Each block was sectioned at 3 μm, and the resulting sections were adhered to glass slides. The slides were stained using a haemotoxylin and alcoholic eosin protocol (see Bojko et al. 2022). The slides were read on a Leica compound microscope and images were taken using a Leica integrated camera.

2.3. Next generation sequencing and bioinformatics

The same 20 crayfish that were prepared for histology, also had corresponding muscle, gill and hepatopancreas preserved in 2 ml of 99 % ethanol. These tissues underwent both DNA and RNA extraction using Wizard extraction kits (Promega), according to manufacturer's protocols. The hepatopancreas of samples C6, C13, and C16 were submitted as individual RNA and DNA extracts for metagenomic and metatranscriptomic analysis. The remaining DNA and RNA extracts from all tissues were pooled into two corresponding batches for sequencing: crayfish samples C1-C10 (excluding C6) were pooled, and crayfish samples C11-C20 (excluding C13 and C16) were pooled, separately for RNA and DNA. This resulted in 5 DNA samples for metagenomics, and 5 RNA samples for metatranscriptomics. The samples were submitted to Novogene, where they underwent library preparation and were sequenced on an Illumina NovaSeq. Each sample provided 10 Gb of paired data, which were delivered to our laboratory for bioinformatic processing.

The files were initially trimmed using Trimmomatic (Bolger et al. 2014; parameters: LEADING:3 TRAILING:3 SLIDINGWINDOW:4:15 MINLEN:36) and then assembled using SPAdes v4.0.0 (Bankevich et al. 2012). The contiguous sequence files from each sample, including samples 3, 13, 16, and the two pooled samples, for both DNA and RNA data, were then used to screen for the presence of symbionts. For the DNA samples, metaxa2 (Bengtsson-Palme et al., 2015) was used to mine out the presence of bacterial and eukaryotic species, by searching for 16S/18S sequences. The DNA datasets were also screened for DNA viruses, using a bespoke DNA virus database, which was built from Refseq DNA viruses on NCBI (August 2024). The RNA datasets were screened for RNA viruses using a bespoke RNA virus database, built from Refseq RNA viruses on NCBI (August 2024). Sequences that indicated possible viral genomes were collected from the contiguous files and completed where necessary. Each viral contig was mapped using the trimmed forward and reverse data in CLC genomics v.12, and then annotated using GeneMarkS (Besemer et al. 2001).

2.4. Phylogenetics and sequence analysis

Viral genomes and their annotations were used to explore their evolutionary origin using blastn, blastp, and blastx. The available protein sequences were used to develop maximum-likelihood phylogenetic trees, all of which underwent 1000 bootstraps and took place using IQ-TREE (Nguyen et al. 2015), after MAFFT alignment. Each viral group was separately explored and the specific details pertaining to each tree are provided in the caption of the relevant figure, including the evolutionary model used, which was predicted in IQ-TREE using Bayesian Information Criterion. Determination of protein function was explored using InterProScan (Jones et al. 2014), and HHpred (Zimmermann et al. 2018), where the following parameters were used to reduce unlikely function assignment: >75 % probability; e-value > $0.1e^{-5}$; p-value <

0.05 (database: PDB_mmCIF70_3_Jan).

Data are available from project code PRJNA1246988 and related biosamples, stored on NCBI.

3. Results

3.1. Protozoan associations

Histological preparation of *P. leptodactylus* tissues resulted in the detection of two symbiont groups: gregarines (Fig. 1A) and ciliated protozoans (Fig. 1B). Gregarines were detected in 15/20 and ciliates in 8/20 individuals The gregarines presented within the gut tissue as elongate single-celled masses, lined against the gut epithelium and bolus (Fig. 1A), but no molecular detection of this species was made in the metagenomic or metatranscriptomic data from HP, gill and muscle tissues. There wasn't evidence of pathology due to the presence of the gregarines alongside the gut epithelial tissues. The ciliated protozoans detected histologically in the gill (Fig. 1B) with no relation to any pathological effect, and were also detected within our metagenomic data, as *Epistylis cambari* (Ciliophora; OQ924989; 61 % cov.; 98.43 % sim.; e-value: 0.0; Table 1). This species was not detected in the HP metagenomic assessments, but was detected in our pooled sample approach which included gill, muscle, and HP together (Table 1).

Metagenomic analysis of DNA extracts from hepatopancreas preps from individuals 6, 13, and 16 did not reveal any detectable protozoan diversity, suggesting a lack of protozoa in this tissue type from these three individuals. However, pooled samples that included both gill and muscle in two batches, 1–10 and 11–20, both revealed further diversity. The pooled sample 11–20 only picked up the *E. cambari* noted above. Pooled sample 1–10 picked up greater diversity, including *Neobodo designis* (Excavata; AY753614; 56 % cov.; 99.45 %; e-value: 0.0) and *Nuclearia moebiusi* (Choanozoa; AF484686; 100 % cov.; 100 % sim.; e-value: 0.0). The presence of these final two species were not detected histologically.

3.2. Putative bacterial associations

In the histological sections, a series of undetermined pathologies within the hepatopancreas were detected in single indidivuals (Fig. 2). Healthy tissue from one individual (Fig. 2A) was compared to four other animals, which presented abnormal pathologies with no specific designation. Putative assignment may involve bacterial or viral origin; however, this is discussed later. Cytoplasmic inclusions were present in specimen 6 (Fig. 2B); however, no bacterial symbiont was detected within the metagenomic data. Agents of viral origin are explored in Section 3.3. Specimen 16 displayed hypertrophic basophilic nuclei (Fig. 2C), and a deep eosinophilic staining hepatopancreatic cytoplasm. Again, molecular analysis via metagenomics did not detect bacterial symbionts in this HP DNA preparation. In specimen 13, the hepatopancreas displayed large clear cytoplasmic inclusions alongside smaller eosinophilic inclusions (Fig. 2D), where typical basophilic staining nuclei of an appropriate size are also seen. Metagenomic data for this sample did pick up one bacterial species, which was *Staphylococcus epidermidis* (Staphylococcaceae; CP052985; 100 % cov.; 100 % sim.; e-value: $6e^{-117}$). Specimen 20 presented small, long green particles within the HP cytoplasm, which were considered unknown in origin. This specimen was a part of the pooled 11–20 batch, which was the source of significant bacterial diversity (Table 2). In addition, pooled batch 1–10 also presented significant bacterial diversity (Table 2).

3.3. Viral associations

A blastx analysis of the metagenomic datasets revealed no presence of complete viral genomes, outside of small fragments with low levels of similarity and e-value support. However, metatranscriptomic analysis of the available RNA sequence data revealed a range of complete and partial RNA viruses within the series of specimens. The complete genomes of eight RNA viruses were identified from metatranscriptomic data from *P. leptodactylus*, alongside a further four partial RNA virus genomes (Suppl. Fig. 1). Complete genomes included five hepe-like viruses, two nodaviruses, and a tombusvirus. Partial genomes included a dicistrovirus, a tombusvirus, and two toti-like viruses. Each virus showed some protein similarity to viruses stored in NCBI (Table 3).

The partial dicistrovirus genome ('Pontastacus leptodactylus Dicistrovirus C16-455'; PlDC16-455) (PV454206) isolated from crayfish C16 was 3547 bp in length (GC% = 51 %), and encoded a partial single polyprotein (826 aa). This protein showed greatest similarity to a polyprotein from 'clirnapec virus 239' (XII42478; sim. 69.24 %; cov. 100 %; e-value: 0.0). InterProScan analysis of the partial polyprotein revealed the following categorised domains: 1–216 region, *Picornavirales* 3C/3C-like protease domain profile (IPR044067); 352–736 region, '*Dicistroviridae* RdRp' (IPR001205). The uncategorised region (217–351) was assessed using HHpred to determine possible function. This analysis determined that this region likely encodes an undetermined transferase (HHpred; probability: 99.84; e-value: $3.1e^{-20}$). The uncategorised region (737——826) was also assessed using HHpred to determine possible function, determining that it may have a hydrolase function, but with low probability (HHpred; probability: 17.61; e-value: 84). Phylogenetic comparison and sequence demarcation analysis of the RdRP region of the novel dicistrovirus, determined that it grouped with viral isolates collected from freshwater bivalves (*Ortmanniana pectorosa*) originating from Virginia (USA), and that it forms a sister branch to the *Cripavirus*

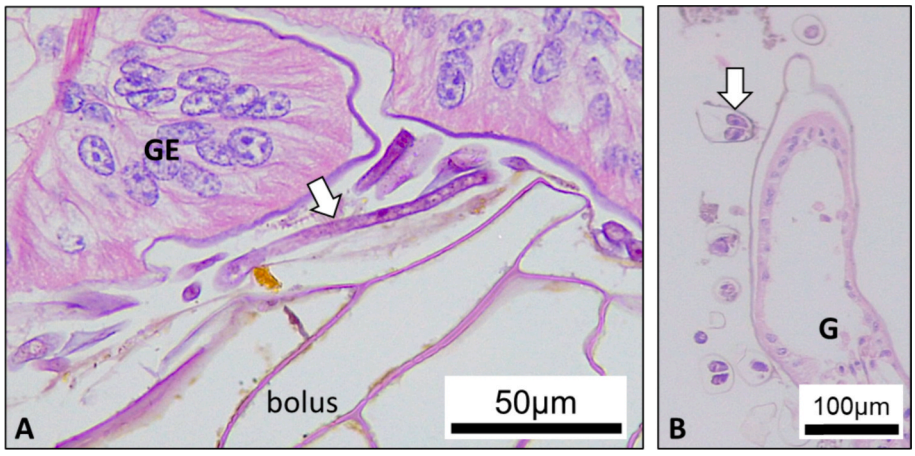

Fig. 1. Protozoa detected in histological section, from *Pontastacus leptodactylus*. A) Gregarine parasites (white arrow) lined against the gut epithelium (GE) and bolus. B) Ciliated protozoa (likely Ciliophora; white arrow), stemming from a single gill lamella (G).

Table 1
Protozoan 18S data derived from the metaxa2 analysis of available NGS datasets collected within this study. The BLAST analysis results are included in this table, highlighting the relevant taxonomy and closest identified organism.

Isolate	Organ	Animal	Length (bp)	Contig coverage	NCBI accession	Similarity (%)	Coverage (%)	E value	Associated species
32,372	Gill/Muscle/HP	C1-10 pool	628	1.324864	AY753614	99.45	56	0.0	*Neobodo designis*
82	Gill/Muscle/HP	C1-10 pool	2597	16.96123	OQ924989	98.43	61	0.0	*Epistylis cambari*
154,056	Gill/Muscle/HP	C1-10 pool	354	1.054152	AF484686	100.00	100	0.0	*Nuclearia moebiusi*
129	Gill/Muscle/HP	C11-20 pool	2597	5.115136	OQ924989	98.43	61	0.0	*Epistylis cambari*

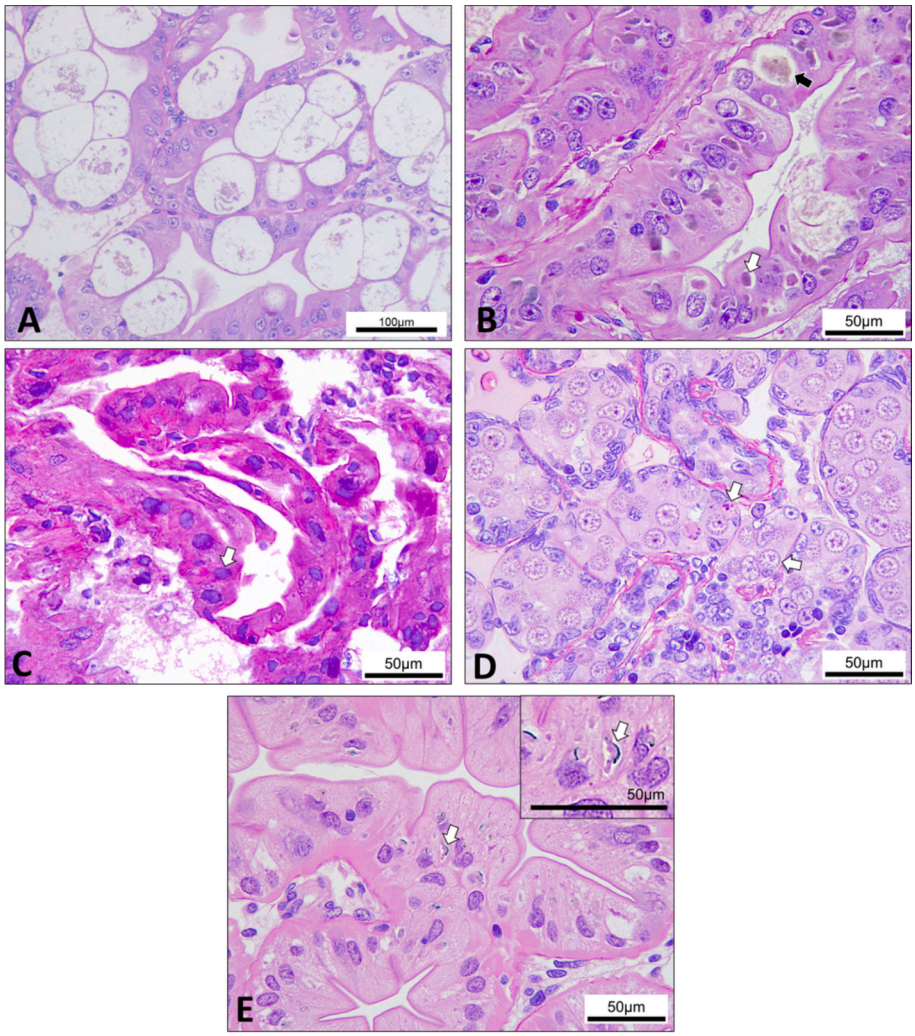

Fig. 2. Various unclassified pathologies located in the hepatopancreas of *Pontastacus leptodactylus* under haemotoxylin and eosin staining, where each was only observed once in our 20-crayfish sample. A) A view of a healthy 'normal' hepatopancreas for comparison. B) Basophilic cytoplasmic inclusions within the hepatopancreatocytes (white arrow), which may develop further to result in cell degradation (black arrow). C) Heavily degraded hepatopancreas with hypertrophic basophilic nuclei in the hepatopancreas (white arrow). D) Large cytoplasmic inclusions in the hepatopancreas appear spherical and clear, or as small eosinophilic inclusions (white arrows). E) Green-staining elongate cytoplasmic inclusions within the hepatopancreas. (For interpretation of the references to colour in this figure legend, the reader is referred to the web version of this article.)

genus within the *Dicistroviridae* (Fig. 3).

Five hepe-like viruses were identified, one more closely associated with the *Hepelivirales* than the others (Fig. 4), which was termed: '*Pontastacus leptodactylus* Hepevirus C13-319′ (PlHC13-319) (PV454208). This isolate was 7480 bp in length (GC% = 47 %) and encoded two proteins, a polyprotein and a capsid protein (Suppl. Fig. 1). Using InterProScan, the viral polyprotein was identified to have the following functional predictions: region 65–296, methyltransferase (IPR002588); region 1129–1301, viral helicase (IPR027351); region 1493–1799, RdRP (IPR001788). This left two major regions without function clarification: region 297–1128, and region 1302–1492. HHpred prediction of the uncategorised 297–1128 region revealed possible tRNA methyltransferase (HHPred; probability: 99.97; e-value: $3e^{-29}$), and capping enzyme (HHpred; probability: 93.6; e-value: $5e^{-1}$) functions. HHpred revealed no confident output for region 1302–1492. The phylogenetic analysis of this virus among the *Hepevirales*, determined that it clusters within an uncategorised section of the phylogeny, but most closely with the *Alphatetraviridae* (Fig. 4). The phylogenetic lineage it sits within houses aquatic mollusc and crustacean-infecting viruses, and environmental samples, including other viruses derived from crayfish.

Four other "hepe-like" viruses were more closely associated with several "hepe-like" viruses from aquatic arthropods, such as crayfish,

Table 2
A blast results table of the bacterial 16S sequences identified by Metaxa2, from the various NGS datasets collected during this study.

Isolate	Organ	Animal	Length (bp)	Contig coverage	NCBI accession	Similarity (%)	Coverage (%)	E value	Associated species
646,264	Hepatopancreas	C13	234	0.929936	CP052985	100.00	100	6e-117	*Stphyloccocus epidermidis*
10,150	Gill/HP/Muscle	Pooled	823	1.43572	JQ692099	91.75	96	0.0	*Flavobacterium terrigena*
					FJ718901	94.33	96	0.0	Uncultured bacterium clone
102,633	Gill/HP/Muscle	Pooled	160	2.01548	MH838009	91.25	100	2e-52	*Runella aurantiaca*
					LR636054	100.00	100	5e-76	Uncultured bacterium
181,617	Gill/HP/Muscle	Pooled	260	1.403846	MW142058	100.00	100	2e-131	*Xanthomonas maliensis*
190,139	Gill/HP/Muscle	Pooled	332	2.078431	KF228157	96.32	98	7e-148	*Nitrosomonas oligotropha*
					EU224342	98.12	96	1e-154	Uncultured bacterium clone 4D
228,968	Gill/HP/Muscle	Pooled	314	1.236287	OK342099	93.65	100	6e-128	*Sediminibacterium* sp.
					KX652468	94.90	100	1e-134	Uncultured bacterium clone OTU 61
28,251	Gill/HP/Muscle	Pooled	677	1.041667	CP042433	96.41	76	3e-69	*Flavisolibacter ginsenosidimutans*
2983	Gill/HP/Muscle	Pooled	1457	1.906166	KX505858	96.37	100	0.0	*Rhodoferax lacus*
31,410	Gill/HP/Muscle	Pooled	499	2.342246	PQ782258	100.00	100	0.0	*Pseudomonas fluorescens*
317,378	Gill/HP/Muscle	Pooled	284	1.057971	OR136292	99.65	100	6e-143	*Rhizobacter profundi*
344,660	Gill/HP/Muscle	Pooled	277	1.825000	AB355702	100.00	100	9e-141	*Thermomonas brevis*
370,875	Gill/HP/Muscle	Pooled	272	1.497436	NR074303	99.13	84	9e-111	*Leadbetterella byssophila*
386,952	Gill/HP/Muscle	Pooled	269	1.161458	MT910335	98.14	100	5e-128	*Microvirga* sp.
387,633	Gill/HP/Muscle	Pooled	269	1.119792	PP341839	100.00	100	2e-136	*Tabrizicola* sp.
429,055	Gill/HP/Muscle	Pooled	259	0.886486	MW486538	98.07	100	2e-122	*Chryseobacterium* sp.
454,119	Gill/HP/Muscle	Pooled	258	0.839779	CP034328	91.63	82	4e-75	*Tabrizicola piscis*
					CP136571	98.21	43	1e-45	*Fuscovulum* sp.
494,379	Gill/HP/Muscle	Pooled	252	0.834286	CP016592	97.24	100	9e-116	*Ketogulonicigenium*
578,718	Gill/HP/Muscle	Pooled	241	0.890244	AB920567	100.00	100	8e-121	*Arthrobacter alpinus*
620,735	Gill/HP/Muscle	Pooled	236	1.377358	NR064420	99.15	100	1e-114	Haliscomenobacter hydrossis
64,403	Gill/HP/Muscle	Pooled	467	1.241026	CP030850	96.35	77	3e-162	*Runella rosea*
659,587	Gill/HP/Muscle	Pooled	232	1.412903	KX981406	86.70	100	4e-64	*Niastella* sp.
					LR637787	97.84	100	2e-107	Uncultured bacterium partial
683,464	Gill/HP/Muscle	Pooled	230	0.954248	EF540472	98.91	80	3e-85	*Flavobacterium* sp.
					KC255331	99.51	88	5e-98	Uncultured bacterium clone GMM_40
685,155	Gill/HP/Muscle	Pooled	135	0.856209	MN620434	100.00	100	3e-62	*Thermomonas* sp.
86,231	Gill/HP/Muscle	Pooled	317	0.959538	CP060007	97.48	100	1e-149	*Lacibacter sediminis*
9363	Gill/HP/Muscle	Pooled	852	2.231717	CP015225	93.15	100	0.0	*Pseudomonas fluorescens*
110,442	Gill/HP/Muscle	Pooled	351	0.532847	OQ359397	94.17	87	3e-127	*Simplicispira piscis*
15,946	Gill/HP/Muscle	Pooled	461	0.854975	JN679215	93.51	83	9e-158	*Terrimonas* sp.
27,873	Gill/HP/Muscle	Pooled	533	0.791667	NR148792	94.65	98	0.0	*Lampropedia cohaerens*
289,926	Gill/HP/Muscle	Pooled	267	0.768421	CP042582	93.55	52	8e-42	*Hypericibacter adhaerens*
					HQ114192	100.00	49	1e-59	Uncultured bacterium clone
440,529	Gill/HP/Muscle	Pooled	151	0.790123	CP002104	100.00	100	5e-71	*Gardnerella vaginalis*
515,085	Gill/HP/Muscle	Pooled	229	0.789474	PP345989	93.39	99	5e-88	*Flavobacterium granuli*
68,997	Gill/HP/Muscle	Pooled	400	0.804954	AM492750	97.20	63	7e-114	*Flavobacterium hercynium*
					CP038810	87.68	100	1e-125	*Flavobacterium sangjuense*

crab, and octopus (Fig. 5; Table 3; Suppl. Fig. 1). The four similar viruses ranged in length between 11,018 and 11,236 bp (GC% range of 48 %–50 %), and were derived from two crayfish (C13 and C16) in our study. Viruses 'Pontastacus leptodactylus Hepevirus C16-9' (PlHC16-9) (PV454211) and 'Pontastacus leptodactylus Hepevirus C13-376' (PlHC13-376) (PV454209) were 99.9 % similar at the nucleotide level and encoded six open reading frames (ORFs); whereas viruses 'Pontastacus leptodactylus Hepevirus C16-8' (PlHC16-8) (PV454210) and 'Pontastacus leptodactylus Hepevirus C13-48' (PlHC13-48) (PV454207) were 99.63 % similar at the nucleotide level and encoded seven ORFs; indicating two groups of similar viruses from two individuals (Fig. 5). For PlHC16-9 and PlHC13-376, the Polyprotein region 175–360 encoded a methyltransferase (IPR002588); and region 1541–1774 encoded a helicase (IPR027351). ORF2 encoded the viral RdRP and ORF3 encoded a transmembrane protein. ORF4-6 had an undetermined function. For PlHC16-8 and PlHC13-48, the Polyprotein region 177–362 encoded a methyltransferase (IPR002588); and region 1541–1774 encoded a helicase (IPR027351). ORF2 encoded the viral RdRP. ORF3-5 all encoded transmembrane proteins. ORF6 and ORF7 had an undetermined function. HHpred analysis did not identify confident predictions for function for the uncharacterised polyprotein regions or ORFs. The phylogenetic tree including these four novel viruses grouped them with other crayfish-infecting viruses, in a lineage separate from those that infect crab and octopus (Fig. 5).

Two distinct nodaviruses were sequenced from the same crayfish specimen (C13). These viruses were termed '*Pontastacus leptodactylus* alphanodavirus C13-3553′ (PlAC13-3553) (PV454212) and '*Pontastacus leptodactylus* alphanodavirus C13-3555′ (PlAC13-3555) (PV454213). Both encoded a single polyprotein and consisted of 3113 bp (GC% = 40 %) and 3210 bp (GC% = 41 %), respectively. The two were 87.32 % similar at the nucleotide level. The polyprotein encoded by the two viruses exhibited the following functional regions (based on PlNC13-3555): 100–241 encoded a methyltransferase (IPR043647); and region 509–749 encoded an RdRP. HHpred prediction of the uncharacterised regions suggested that region 242–508 of the polyprotein is an extension of the RdRP prediction, including a capping enzyme (HHpred; probability: 100; e-value: $1.1e^{-63}$). The remaining region (750–1020) is also an extension of the InterProScan-predicted RdRP site, but specific to transferase function (HHpred; probability: 99.17; e-value: $5.3e^{-11}$). Phylogenetic analysis using the entire polyprotein determined that the two nodaviruses branch closely together, on a sister branch to the Leuven nodavirus (QZZ63349) and an environmental sample (XKB76444; Fig. 6). *Alphanodavirus flockense* branches at the base of the cluster containing the two *P. leptodactylus*-infecting nodaviruses (support: 67 %). This cluster also contains a nodavirus sequenced from a freshwater bivalve (Chemarfal virus 256; WPR18356; Fig. 6).

Two tombusvirus sequences were identified from animal C13. A partial genome encoding two ORFs is termed 'Pontastacus leptodactylus tombusvirus C13-5563′ (PlTC13-5563) (PV454215), which was 2518 bp in length (GC% = 39 %). A complete viral genome containing four ORFs

Table 3
RNA virus proteins are included in this table, alongside their blastp comparison result. The table indicates the most closely related known virus, identified prior to this study.

Virus Name	ORF	Animal	Length (aa)	NCBI accession	Similarity (%)	Coverage (%)	E value	Associated taxon
Pontastacus_leptodactylus_Dicistrovirus_C16-455	1	C16	826	XII42478	69.24	100	0.0	clirnapec virus 239
Pontastacus_leptodactylus_Hepevirus_C13-48	1	C13	1897	CAJ2444841	53.64	31	2e-180	*Astacus astacus hepevirus*
Pontastacus_leptodactylus_Hepevirus_C13-48	2	C13	471	CAJ2358127	74.57	99	0.0	*Astacus astacus hepevirus*
Pontastacus_leptodactylus_Hepevirus_C13-48	3	C13	254	CAJ2444836	54.00	98	6e-89	*Astacus astacus hepevirus*
Pontastacus_leptodactylus_Hepevirus_C13-48	4	C13	95	No significant similarity found				
Pontastacus_leptodactylus_Hepevirus_C13-48	5	C13	107	No significant similarity found				
Pontastacus_leptodactylus_Hepevirus_C13-48	6	C13	415	CAJ2444837	72.02	99	0.0	*Astacus astacus hepevirus*
Pontastacus_leptodactylus_Hepevirus_C13-48	7	C13	155	CAJ2444838	56.21	99	1e-51	*Astacus astacus hepevirus*
Pontastacus_leptodactylus_Hepevirus_C13-319	1	C13	1855	WAY16406	50.30	9	3e-40	*Hepelivirales* sp.
Pontastacus_leptodactylus_Hepevirus_C13-319	2	C13	540	WAY16407	43.37	83	1e-106	*Hepelivirales* sp.
Pontastacus_leptodactylus_Hepevirus_C13-376	1	C13	1894	CAJ2444841	64.79	91	0.0	*Astacus astacus hepevirus*
Pontastacus_leptodactylus_Hepevirus_C13-376	2	C13	550	CAJ2358127	81.93	100	0.0	*Astacus astacus hepevirus*
Pontastacus_leptodactylus_Hepevirus_C13-376	3	C13	202	CAJ2358133	71.29	100	3e-94	*Astacus astacus hepevirus*
Pontastacus_leptodactylus_Hepevirus_C13-376	4	C13	418	CAJ2358134	65.16	100	0.0	*Astacus astacus hepevirus*
Pontastacus_leptodactylus_Hepevirus_C13-376	5	C13	123	No significant similarity found				
Pontastacus_leptodactylus_Hepevirus_C13-376	6	C13	169	CAJ2358130	53.21	92	8e-52	*Astacus astacus hepevirus*
Pontastacus_leptodactylus_Hepevirus_C16-8	1	C16	1897	CAJ2444841	53.64	31	2e-180	*Astacus astacus hepevirus*
Pontastacus_leptodactylus_Hepevirus_C16-8	2	C16	471	CAJ2358127	74.57	99	0.0	*Astacus astacus hepevirus*
Pontastacus_leptodactylus_Hepevirus_C16-8	3	C16	254	CAJ2444836	54.00	98	6e-89	*Astacus astacus hepevirus*
Pontastacus_leptodactylus_Hepevirus_C16-8	4	C16	95	No significant similarity found				
Pontastacus_leptodactylus_Hepevirus_C16-8	5	C16	107	No significant similarity found				
Pontastacus_leptodactylus_Hepevirus_C16-8	6	C16	415	CAJ2444837	72.02	99	0.0	*Astacus astacus hepevirus*
Pontastacus_leptodactylus_Hepevirus_C16-8	7	C16	155	CAJ2444838	56.21	99	1e-51	*Astacus astacus hepevirus*
Pontastacus_leptodactylus_Hepevirus_C16-9	1	C16	1894	CAJ2444841	64.79	91	0.0	*Astacus astacus hepevirus*
Pontastacus_leptodactylus_Hepevirus_C16-9	2	C16	550	CAJ2358127	81.57	100	0.0	*Astacus astacus hepevirus*
Pontastacus_leptodactylus_Hepevirus_C16-9	3	C16	202	CAJ2358133	71.29	100	3e-94	*Astacus astacus hepevirus*
Pontastacus_leptodactylus_Hepevirus_C16-9	4	C16	418	CAJ2358134	65.16	100	0.0	*Astacus astacus hepevirus*
Pontastacus_leptodactylus_Hepevirus_C16-9	5	C16	123	No significant similarity found				
Pontastacus_leptodactylus_Hepevirus_C16-9	6	C16	169	CAJ2358130	53.21	92	8e-52	*Astacus astacus hepevirus*
Pontastacus_leptodactylus_Nodamuravirus_C13-3553	1	C13	967	XKB76444	80.60	99	0.0	*Nodamuvirus*
Pontastacus_leptodactylus_Nodamuravirus_C13-3555	1	C13	1031	XKB76444	80.74	100	0.0	*Nodamuvirus*
Pontastacus_leptodactylus_Tombusvirus_C13-873	1	C13	260	YP_009336878	30.77	45	3e-07	Hubei tombus-like virus
Pontastacus_leptodactylus_Tombusvirus_C13-873	2	C13	409	UBJ25992	28.40	37	5e-05	Sichuan mosquito tombus-like virus
Pontastacus_leptodactylus_Tombusvirus_C13-873	3	C13	502	UBJ25993	58.08	67	5e-142	Sichuan mosquito tombus-like virus
Pontastacus_leptodactylus_Tombusvirus_C13-873	4	C13	627	XKB76289	41.41	16	7e-16	*Tombusviridae*
Pontastacus_leptodactylus_Tombusvirus_C13-5563	1	C13	296	WRQ65157	27.78	49	8e-07	*Tombusviridae*
Pontastacus_leptodactylus_Tombusvirus_C13-5563	2	C13	465	WRQ65158	42.70	78	9e-80	*Tombusviridae*
Pontastacus_leptodactylus_Totivirus_C16-10330	1	C16	268	UHS72454	51.06	18	3e-07	*Totiviridae*
Pontastacus_leptodactylus_Totivirus_C16-11810	1	C16	248	UHS72490	53.56	94	2e-66	*Totiviridae*

is termed 'Pontastacus leptodactylus tombusvirus C13-873′ (PlTC13-873) (PV454214), which was 5600 bp in length (GC% = 41 %). The proteins encoded by the two viruses show varied levels of similarity to other tombusviruses (BLAST TABLE). The two ORFs encoded by PlTC13-5563 consist of a transmembrane protein (ORF1) and an RdRP (ORF2) according to InterProScan. The complete tombusvirus genome (PlTC13-873) encoded four ORFs (Suppl. Fig. 1), which appear to function in the following ways based on InterProScan and HHpred predictions: ORF1, undetermined; ORF2, undetermined; ORF3 encodes an RdRP; and ORF4 encodes a peptidase A21 (IPR005313). The tombusvirus phylogeny determined that the complete and partial viruses sequenced in this study group separately across the *Tombusviridae* (Fig. 7). PlTC13-5563 groups with other crustacean and mollusc-infecting tombusviruses from aquatic environments, most closely associated with the *Regressovirinae* and *Calvusvirinae*. PlTC13-873 groups in a different part of the tree, alongwith related viruses from mosquito, bird, and molluscan origin (Fig. 7).

Finally, two genomic fragments with greatest similarity to the *Totiviridae* (Table 3) (PV454216) (PV454217) were isolated from sample C16. These two fragments are considered partial sequences of a viral polyprotein and consisted of 805 bp and 746 bp.

4. Discussion

This study explores symbiotic organisms in the only known population of non-native narrow-clawed crayfish, *P. leptodactylus* in West Yorkshire, UK. Invasive crayfish pose a significant threat to native crayfish through both competition and disease (Everard et al. 2009) and this recently established population could pose a risk to native white-claw crayfish populations, with the nearest known population of the native species only ten km downstream (WoC ID: WK9180; for *A. pallipes*, observation date: 2022; Ion et al. 2024). Information on the disease profile of this population will assist in further elucidating the level of risk presented.

4.1. Symbionts in an early invading population of narrow-clawed crayfish

Previous records associate a range of symbionts with *P. leptodactylus* (reviewed in Bojko et al. 2021). Our study found a lack of nudiviruses, Microsporidia, Fungi, some protozoans (including *Psorospermium*), and Metazoa, such as trematodes, from the UK population, which are present in *P. leptodactylus* in its native range (Bojko et al. 2021). The absence of these pathogens may reflect enemy release (Williamson, 1996; Keane &

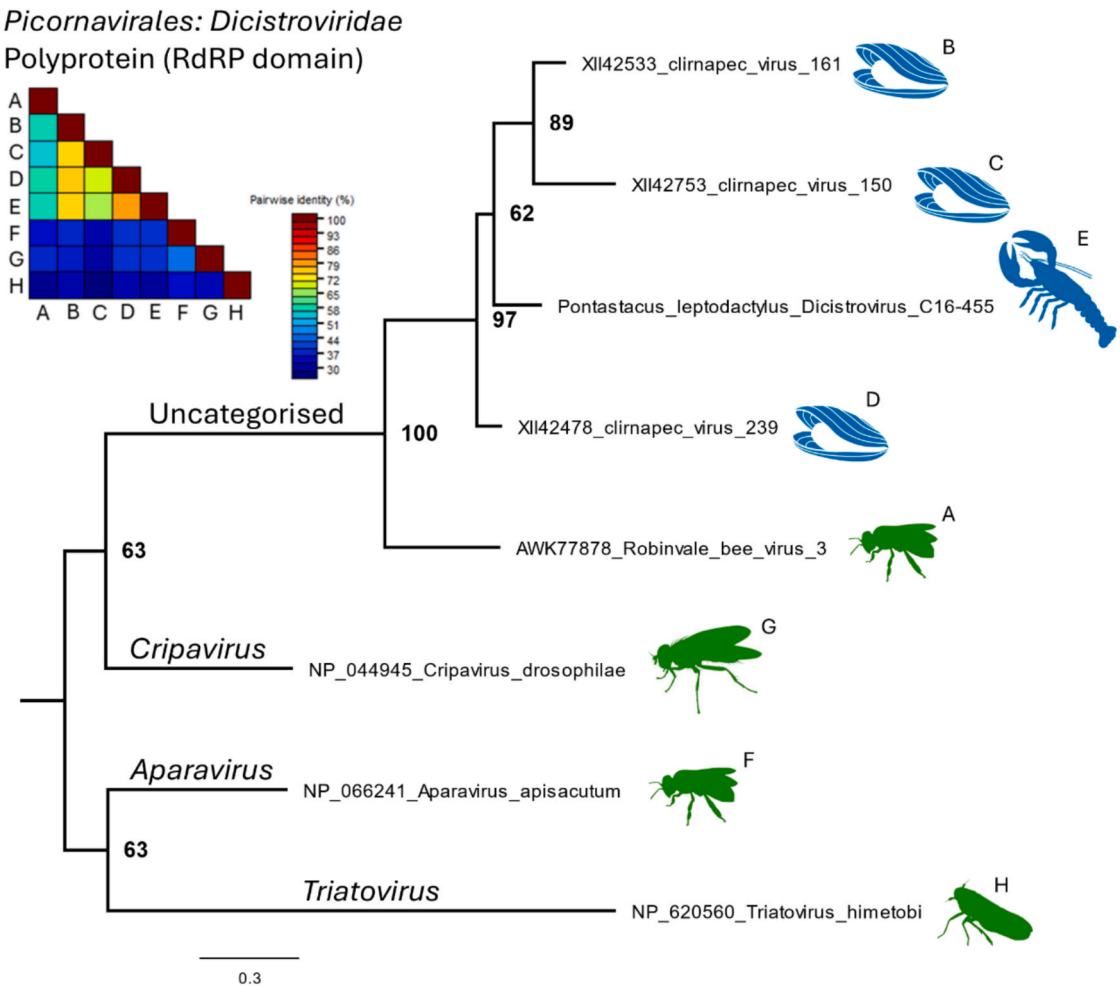

Fig. 3. A maximum-likelihood phylogenetic tree representing the phylogenetic position of a partial dicistrovirus genome from *Pontastacus leptodactylus*, based on the RNA-dependent RNA polymerase (RdRP) region of the polyprotein. The tree is midpoint rooted. The tree includes 8 viral isolates, including representatives from the *Triatovirus*, *Aparavirus*, and *Cripavirus*. The tree is based on the best-fit model: LG + G4, chosen according to Bayesian information criterion. The original alignment included 340 columns, 316 distinct patterns, 152 parsimony-informative sites, 130 singleton sites, and 58 constant sites. The tree was developed using IQ-TREE and annotated using FigTree. In addition, a sequence demarcation plot is presented, highlighting the approximate percent similarity between the RdRP regions of the viruses included in the analysis. Small animal icons are present to indicate the host and they are coloured in either green (terrestrial) or blue (aquatic) to represent their environmental origin. (For interpretation of the references to colour in this figure legend, the reader is referred to the web version of this article.)

Crawley, 2002; Colautti et al. 2004; Miura and Torchin, 2023), where the founding population 'escaped' pathogens as a results of stochastic and selective pressures during invasion. However, we did detect several protozoans, bacterial species, and RNA viruses.

The protozoan, *E. cambari*, infests the gill filaments of crayfish (Abd El-Moaty et al. 2016), with no known negative effects; however, high burden of *Epistylis* sp. has been associated with lower concentrations of dissolved oxygen within a waterbody, potentially indicating increased organic matter decomposition (Quaglio et al. 2004). Ciliated protozoa (*Epistylis* sp., etc.) were commonly noted in the gill histology, and are likely commensal associations. The Protozoa, *Neobodo designis and Nuclearia moebiusi* may also be considered commensal associates and are commonly found in aquatic biomes (Chavez-Dozal et al. 2013; Gabaldón et al., 2022). Our detection of these two species increases their known habitation to crayfish, as symbionts.

Of the bacteria that we detected, two show genetic similarity to opportunistic human pathogens: *Gardnerella vaginalis* and *Staphylococcus epidermidis*. *Gardnerella vaginalis* has been linked to sexually transmitted infections and public health complications (Schwebke et al. 2014). *Staphylococcus epidermidis* colonises human skin (Otto, 2012). It is likely that both of these bacteria have entered the waterbody, and crayfish, through either human waste or bathing. The other bacteria observed in this study likely form a part of the more natural crayfish microbiome, within UK waters. *Xanthomonas maliensis* (Triplett et al. 2015), *Pseudomonas fluorescens* (Rainey, 1999) and *Leadbetterella byssophila* (Weon et al., 2005) have all previously been found in vegetation and agricultural samples with no notable effects on their host or environment. *Thermomonas brevis* (Mergaert et al. 2003) and *Haliscomenobacter hydrossis* (Daligault et al. 2011) have both been found in water samples with no notable effects, and *Arthrobacter alpinus* has previously been found in soil samples, with no notable effects (Zhang et al. 2010). We believe that these species are likely to be commensal or mutualists with regard to their crayfish host.

We did not identify any DNA viruses from metagenomic data collected from our samples, despite previous detection of viruses in this species (Petersen et al. 2024). However, we did sequence and identify several RNA viruses from the population. This included a dicistrovirus, several hepe-like viruses (~*Hepelivirales*), nodaviruses, tombusvirus, and a totivirus. For the majority of these viruses, this is their first detection and knowledge of their pathological effect is limited.

The Pontastacus_leptodactylus_Dicistrovirus_C16-455 and partial totivirus sequences were detected only in specimen 16, which had an hepatopancreatic pathology visible in Fig. 2C. No other hepatopancreas from specimens in our sample set presented this way, and follow-up of

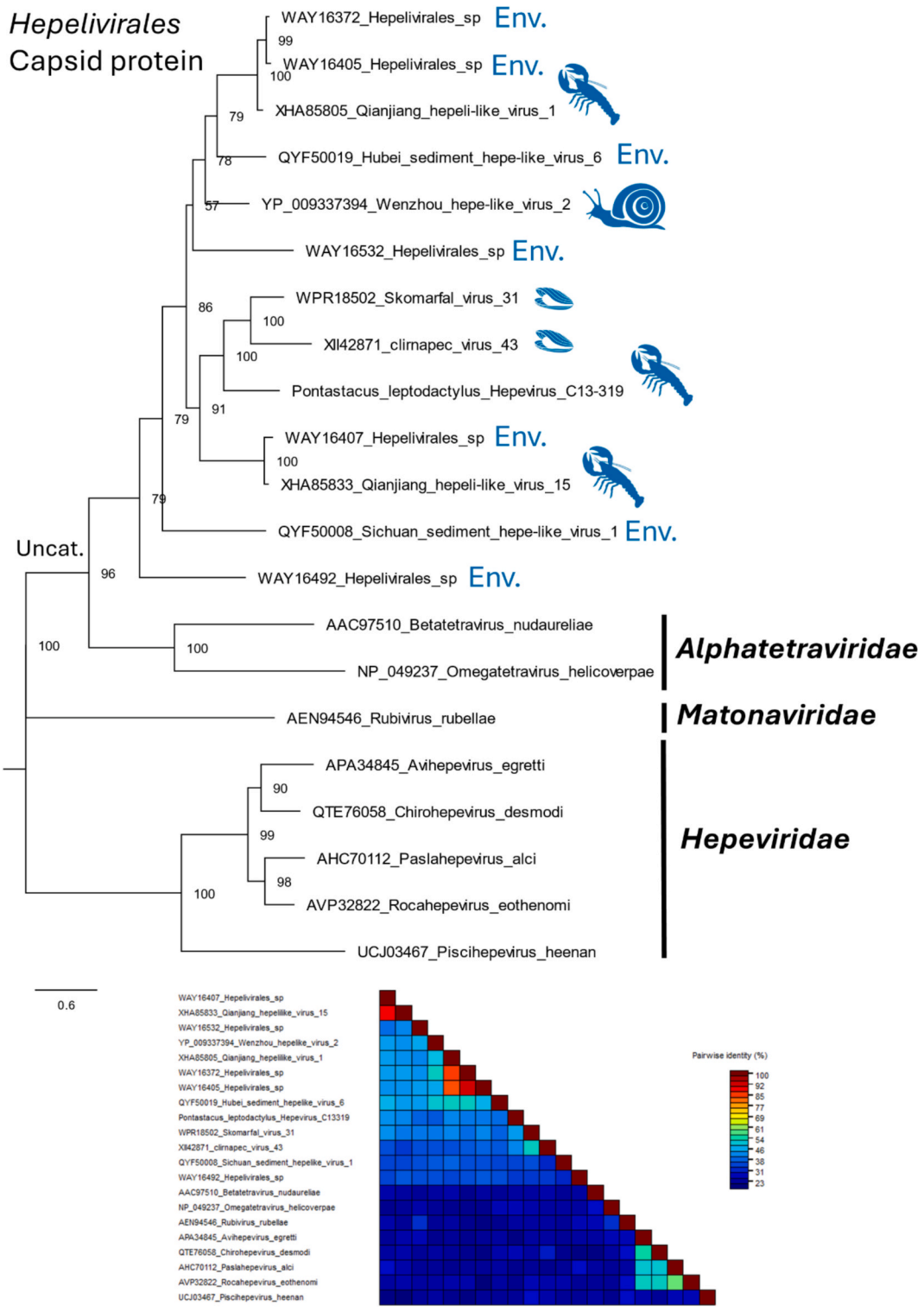

Fig. 4. A maximum-likelihood phylogenetic tree representing the phylogenetic position of a new hepe-like virus from *Pontastacus leptodactylus* within the *Hepelivirales*, based on the capsid protein. The tree is midpoint rooted. The tree includes representatives from the *Alphatetraviridae*, *Matonaviridae*, and *Hepeviridae*. The tree is based on the best-fit model: LG + F + I + G4, chosen according to Bayesian information criterion. The original alignment has 21 sequences with 1329 columns, 1029 distinct patterns, 624 parsimony-informative sites, 291 singleton sites, and 413 constant sites. The tree was developed using IQ-TREE and annotated using FigTree. In addition, a sequence demarcation plot is presented, highlighting the approximate percent similarity between the capsid proteins of the viruses included in the analysis. Small animal icons are present to indicate the host and they are coloured in blue to represent their aquatic origin. Inclusion of the 'Env.' Term after some isolates indicates an environmental sample. (For interpretation of the references to colour in this figure legend, the reader is referred to the web version of this article.)

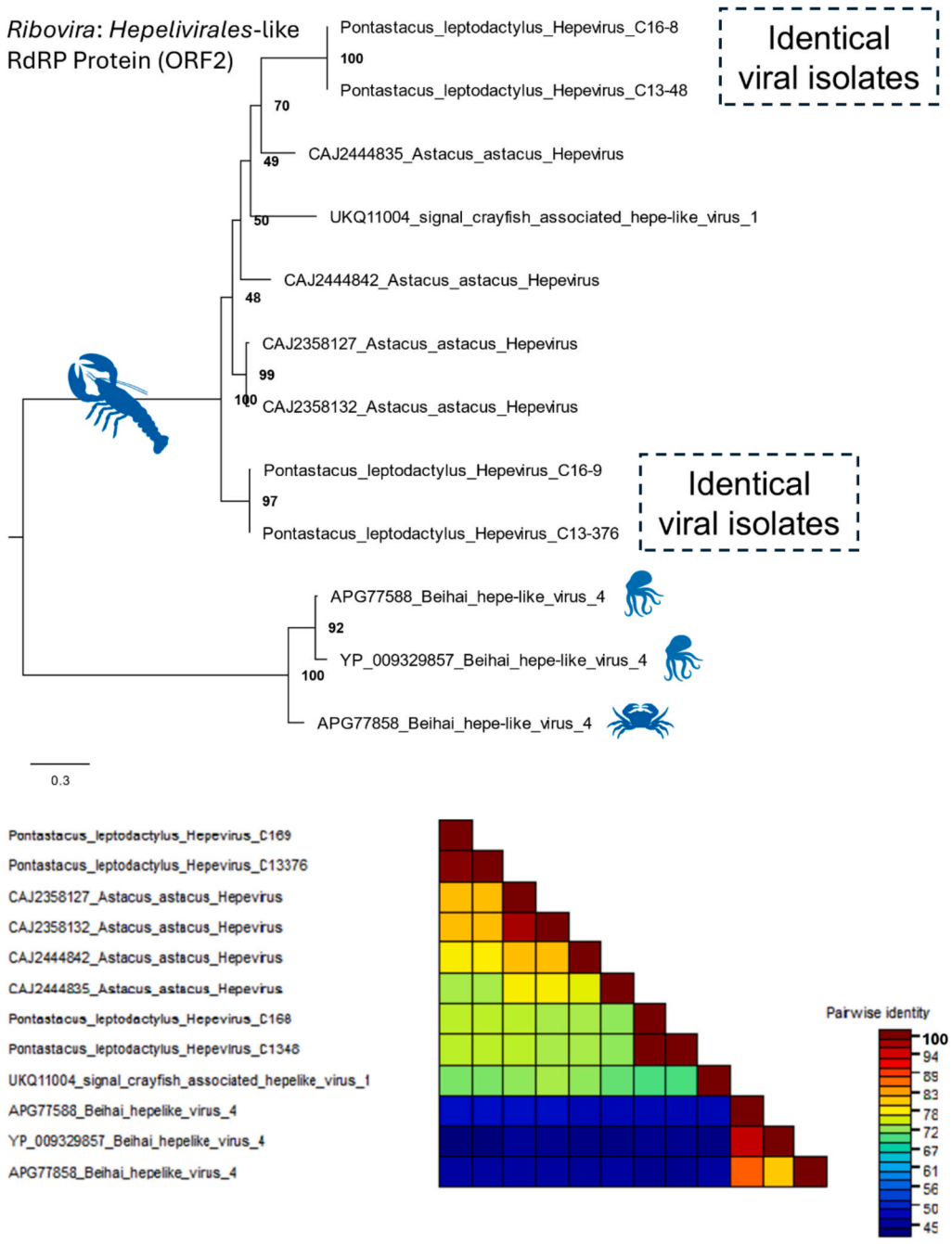

Fig. 5. A maximum-likelihood phylogenetic tree representing the phylogenetic position of several *Riboviria* (*Hepevirales*-like) viruses from *Pontastacus leptodactylus*, based on the RNA-dependent RNA polymerase (RdRP) protein (open reading frame 2). The tree is midpoint rooted. The tree includes 12 viral isolates, including representatives from NCBI, but with no specific taxonomic detail provided to date by the ICTV. The tree is based on the best-fit model: LG + G4, chosen according to Bayesian Information Criterion. The original alignment includes 693 columns, 435 distinct patterns, 308 parsimony-informative sites, 70 singleton sites, 315 constant sites. The tree was developed using IQ-TREE and annotated using FigTree. In addition, a sequence demarcation plot is presented, highlighting the approximate percent similarity between the RdRP proteins of the viruses included in the analysis. Small animal icons are present to indicate the host and they are coloured in blue to represent their aquatic origin. (For interpretation of the references to colour in this figure legend, the reader is referred to the web version of this article.)

this pathology will be valuable to gain further detail on whether one of these virus groups drove such hepatopancreatic presentation in the histological section. Dicistroviruses have previously been shown to cause mortality in arthropods (Sun et al., 2024) and such a discovery may have relevance to crayfish population control.

Pontastacus_leptodactylus_Hepevirus_C13-319 had a unique genome organisation among the hepe-like viruses we detected, with two open reading frames, and was only detected in specimen 13. Two nodavirus-like genomes were specifically detected in specimen 13: Pontastacus_leptodactylus_Nodamuravirus_C13-3553 and Pontastacus_leptodactylus_Nodamuravirus_C13-3555, as was a tombusvirus (Pontastacus_leptodactylus_Tombusvirus_C13-873). It is more difficult in this situation to determine if these viruses were involved in the pathology in the hepatopancreas of specimen 13 (Fig. 2D). In-situ hybridisation methods may aid to untangle this detail in future studies.

The detail provided above gives an overview of the symbiotic community housed within invasive *P. leptodactylus* at a freshwater site in West Yorkshire. They house a broad array of protozoans (gregarines;

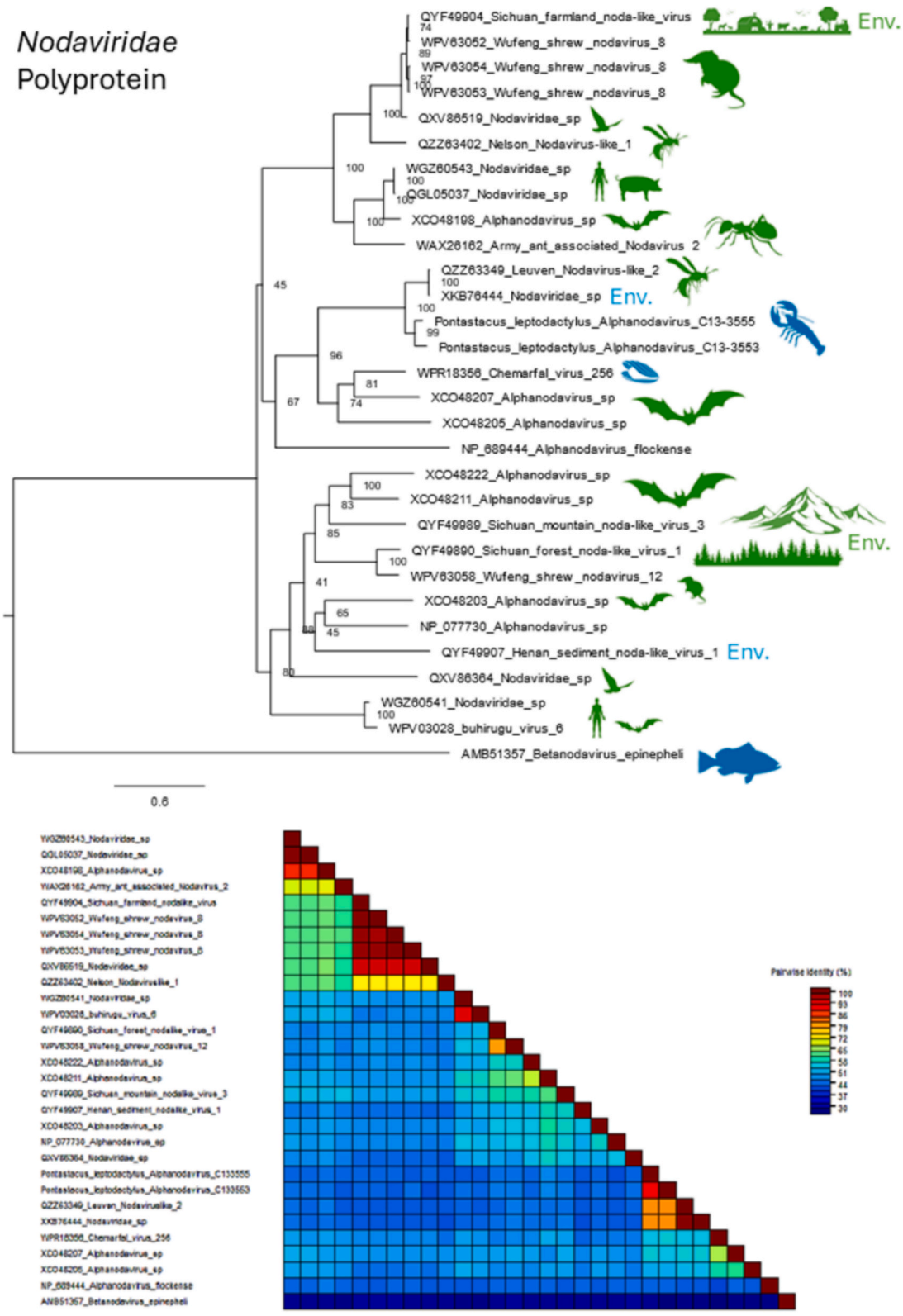

Fig. 6. A maximum-likelihood phylogenetic tree representing the phylogenetic position of two new nodaviruses from *Pontastacus leptodactylus*, based on a whole polyprotein alignment. The tree is midpoint rooted. The tree includes representatives from the *Betanodavirus* and *Alphanodavirus* genera. The tree is based on the best-fit model: LG + I + G4, chosen according to Bayesian information criterion. The original alignment has 30 sequences with 1250 columns, 1138 distinct patterns, 824 parsimony-informative sites, 233 singleton sites, and 193 constant sites. The tree was developed using IQ-TREE and annotated using FigTree. In addition, a sequence demarcation plot is presented, highlighting the approximate percent similarity between the polyproteins of the viruses included in the analysis. Small animal icons or environmental icons are present to indicate the host or origin of the sample, and they are coloured in either green (terrestrial) or blue (aquatic) to represent their environmental origin. Inclusion of the 'Env.' Term after some isolates indicates an environmental sample – green refers to terrestrial, blue refers to aquatic. (For interpretation of the references to colour in this figure legend, the reader is referred to the web version of this article.)

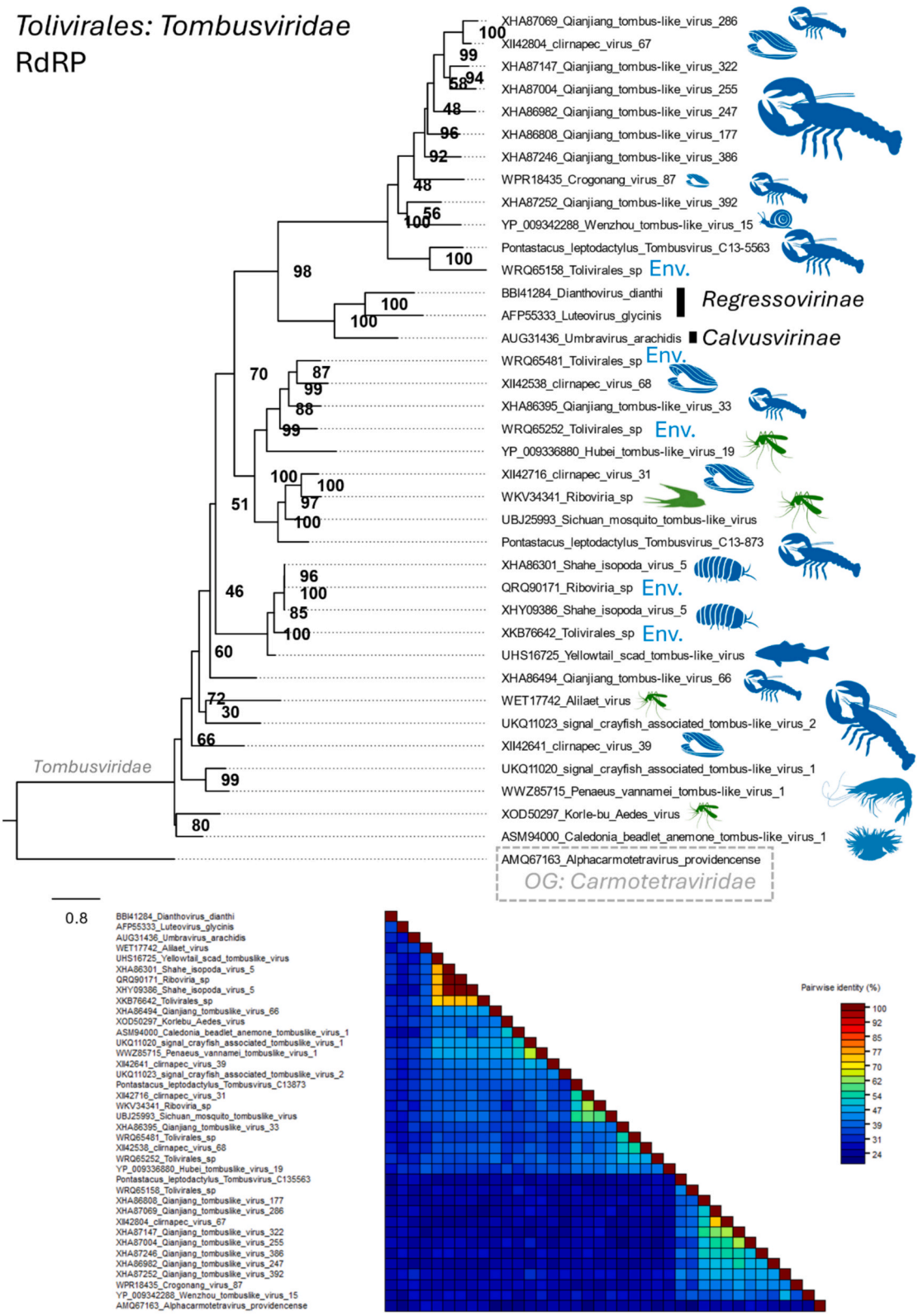

Fig. 7. A maximum-likelihood phylogenetic tree representing the phylogenetic position of two new tombusviruses from *Pontastacus leptodactylus*, based on RNA-dependent RNA polymerase protein alignment. The tree includes representatives from the *Regressovirinae* and *Calvusvirinae*, and includes a member of the *Carmotetraviridae* as an out-group. The tree is based on the best-fit model: LG + I + G4, chosen according to Bayesian information criterion. The original alignment has 38 sequences with 1399 columns, 1261 distinct patterns, 625 parsimony-informative sites, 506 singleton sites, and 268 constant sites. The tree was developed using IQ-TREE and annotated using FigTree. In addition, a sequence demarcation plot is presented, highlighting the approximate percent similarity between the polyproteins of the viruses included in the analysis. Small animal icons or environmental icons are present to indicate the host or origin of the sample, and they are coloured in either green (terrestrial) or blue (aquatic) to represent their environmental origin. Inclusion of the 'Env.' Term after some isolates indicates an environmental sample – green refers to terrestrial, blue refers to aquatic. (For interpretation of the references to colour in this figure legend, the reader is referred to the web version of this article.)

Table 1), bacteria (Table 2), and RNA viruses (Table 3), but lack microsporidians, DNA viruses, and common metazoan groups, like trematodes and acanthocephalans.

4.2. Virological novelties

Each of the viral genomes that we have uncovered will require formal ratification by the International Committee on Taxonomy of Viruses (ICTV). We estimate that the complete viral genomes we provide herein will increase known diversity within the *Riboviria*, with specific detail relevant to the *Nodaviridae*, *Dicistroviridae*, *Hepelivirales*, and *Tombusviridae*, alongside of partial genomes for viruses that require follow-up study (i.e. *Totiviridae*).

In each of our phylogenetic trees (Figs. 3-7), we have provided relative ICTV accepted species as anchor points to determine the likely taxonomic relevance of each new discovery. In all but two cases, the viruses we have identified sit outside of current taxonomic boundaries and, for the majority, have only been comparable using predicted protein sequence data. The nodavirus-like genomes that we sequenced from specimen 13 are the only viruses with comparable nucleotide similarity to other sequenced viruses, which show ~79 % nucleotide similarity with a nodavirus that had been identified in wasps (Leuven nodavirus; MZ443597). This virus has been seen in the genus *Vespula*, a group of predatory wasps that are also invasive (Remnant et al. 2021) and we highlight that this group is now also associated with aquatic invertebrates alongside terrestrial species. The crayfish nodaviruses appear to group into a lineage of the *Alphanodavirus* genus (Fig. 6), branching with *Alphanodavirus flockense* (aka. 'Flock House virus'), a virus from insects with control applications (Jiang et al. 2023).

In other cases, our viruses group with others emerging from large studies into viral diversity; however, one particularly unique observation is that of the hepe-like viruses, which each encode 6–7 open reading frames (Fig. 5). We provide genomes for four hepe-like viruses, which group with similar viruses only found in crayfish to date (Bačnik et al. 2021 and direct NCBI submissions). The crayfish hosts identified to date are *P. leniusculus* and *A. astacus*. Outside of this group are only three comparable viruses, two from octopi and one from a crab. Our findings here support a unique group of viruses within the crayfish virome that requires further exploration and possibly the erection of a novel taxonomic group as sister to the *Hepelivirales*.

4.3. Conclusions and future directions

Pontastacus leptodactylus in the UK are associated with a diverse range of symbionts. This invader appears to have rapidly acquired these symbioses from the UK freshwater environment during a short time period (introduced to Boshaw Whams in 2014), but several of these symbionts may have co-invaded along with the founder population. Our approach to screening this invasive population presents a pathway for considering a rapid method to determine symbiont introduction risk via an invasive species, saving cost by pooling tissue nucleotide extracts for individual next generation sequencing runs, with supporting histopathology (following Bojko et al. 2023). We conclude that, despite the population harbouring a diverse array of RNA virus, bacterial, and protozoan symbionts, the population appears to have escaped mortality-inducing groups, such as Microsporidia (Stratton et al., 2024a) and *Bunyavirales* (Grandjean et al. 2019).

CRediT authorship contribution statement

Matthew Harwood: Writing – review & editing, Writing – original draft, Visualization, Validation, Supervision, Software, Resources, Project administration, Methodology, Investigation, Funding acquisition, Formal analysis, Data curation, Conceptualization. **Josie South:** Writing – review & editing, Writing – original draft, Supervision, Investigation, Funding acquisition, Conceptualization. **Alison M. Dunn:** Writing – review & editing, Writing – original draft, Supervision, Conceptualization. **Paul D. Stebbing:** Writing – review & editing, Writing – original draft, Supervision, Conceptualization. **Amy Burgess:** Writing – review & editing, Writing – original draft, Methodology, Conceptualization. **Jamie Bojko:** Writing – review & editing, Writing – original draft, Visualization, Validation, Supervision, Software, Resources, Project administration, Methodology, Investigation, Funding acquisition, Formal analysis, Data curation, Conceptualization.

Declaration of competing interest

The authors declare that they have no known competing financial interests or personal relationships that could have appeared to influence the work reported in this paper.

Acknowledgements

We thank Yorkshire Water for funding this research. MH acknowledges support from the John Henry Garner Scholarship and APEM. JS acknowledges funding from UKRI Future Learers Fellowship [Grant/Award Number: MR/X035662/1].

Appendix A. Supplementary data

Supplementary data to this article can be found online at https://doi.org/10.1016/j.jip.2025.108458.

References

Abd El-Moaty, S.M., Sharaf, H.M., Khalil, A.E.M., Ahmed, S.S., 2016. Survey on the parasites infested crayfish Procambarus clarkii, Girard, 1852 (Crustacea, Cambaridae) in Egypt. J. Biosci. App. Res. 2 (6), 395–400. https://doi.org/10.21608/jbaar.2016.108531.

Anaya, C., 2021. First Record of Psorospermium sp. (Class: Mesomycetozoea) in Northern Clearwater crayfish Faxonius propinquus Girard, (Decapoda: Cambaridae) from Michigan, USA. Zootaxa 4981 (1), 197–200.

Anderson, L.G., Bojko, J., Bateman, K.S., Stebbing, P.D., Stentiford, G.D., Dunn, A.M., 2021. Patterns of infection in a native and an invasive crayfish across the UK. J. Invertebr. Pathol. 184, 107595.

Bačnik, K., Kutnjak, D., Černi, S., Bielen, A., Hudina, S., 2021. Virome analysis of signal crayfish (*Pacifastacus leniusculus*) along its invasion range reveals diverse and divergent RNA viruses. Viruses 13 (11), 2259.

Bankevich, A., Nurk, S., Antipov, D., Gurevich, A.A., Dvorkin, M., Kulikov, A.S., Pevzner, P.A., 2012. SPAdes: A new genome assembly algorithm and its applications to single-cell sequencing. J. Comput. Biol. 19 (5), 455–477.

Bengtsson-Palme, J., Hartmann, M., Eriksson, K.M., Pal, C., Thorell, K., Larsson, D.G.J., Nilsson, R.H., 2015. METAXA2: improved identification and taxonomic classification of small and large subunit rRNA in metagenomic data. Mol. Ecol. Resour. 15 (6), 1403–1414.

Besemer, J., Lomsadze, A., Borodovsky, M., 2001. GeneMarkS: A self-training method for prediction of gene starts in microbial genomes. Implications for finding sequence motifs in regulatory regions. Nucleic Acids Res. 29 (12), 2607–2618.

Bojko, J., Stentiford, G.D., Stebbing, P.D., Hassall, C., Deacon, A., Cargill, B., Dunn, A.M., 2019. Pathogens of *Dikerogammarus haemobaphes* regulate host activity and survival, but also threaten native amphipod populations in the UK. Dis. Aquat. Organ. 136 (1), 63–78.

Bojko, J., Behringer, D.C., Moler, P., Stratton, C.E., Reisinger, L., 2020. A new lineage of crayfish-infecting Microsporidia: The Cambaraspora floridanus n. gen. n. sp. (Glugeida: Glugeidae) complex from Floridian freshwaters (USA). J. Invertebr. Pathol. 171, 107345.

Bojko, J., Burgess, A.L., Baker, A.G., Orr, C.H., 2021. Invasive non-native crustacean symbionts: Diversity and impact. J. Invertebr. Pathol. 186, 0022–2011. https://doi.org/10.1016/j.jip.2020.107482. ISSN 107482.

Bojko, J., Burgess, A.L., Allain, T.W., Ross, E.P., Pharo, D., Kreuze, J.F., Behringer, D.C., 2022. Pathology and genetic connectedness of the mangrove crab (Aratus pisonii) – a foundation for understanding mangrove disease ecology. Animal Dis. 2 (8). https://doi.org/10.1186/s44149-022-00039-7.

Bojko, J., Collings, A. J., Burgess, A. L., & Goode, J. A. (2023). Diagnosing Invasive Parasites. In: Parasites and Biological Invasions. GB: CABI. p. 8–23.

Bolger, A.M., Lohse, M., Usadel, B., 2014. Trimmomatic: A flexible trimmer for Illumina sequence data. Bioinformatics 30 (15), 2114–2120.

Chavez-Dozal, A., Gorman, C., Erken, M., Steinberg, P.D., McDougald, D., Nishiguchi, M. K., 2013. Predation response of vibrio fischeri biofilms to bacterivorus protists. Appl. Environ. Microbiol. 79. https://doi.org/10.1128/AEM.02710-12.

Colautti, R.I., Ricciardi, A., Grigorovich, I.A., MacIsaac, H.J., 2004. Is invasion success explained by the enemy release hypothesis? Ecol. Lett. 7, 721–733. https://doi.org/10.1111/j.1461-0248.2004.00616.x.

Daligault, H., Lapidus, A., Zeytun, A., Nolan, M., Lucas, S., Del Rio, T.G., Tice, H., Cheng, J.F., Tapia, R., Han, C., Goodwin, L., Pitluck, S., Liolios, K., Pagani, I., Ivanova, N., Huntemann, M., Mavromatis, K., Mikhailova, N., Pati, A., Chen, A., Palaniappan, K., Land, M., Hauser, L., Brambilla, E.M., Rohde, M., Verbarg, S., Göker, M., Bristow, J., Eisen, J.A., Markowitz, V., Hugenholtz, P., Kyrpides, N.C., Klenk, H.P., Woyke, T., 2011. Complete genome sequence of Haliscomenobacter hydrossis type strain (O). Stand. Genomic. Sci. 4 (3), 352–360. https://doi.org/10.4056/sigs.1964579. Epub 2011 Jun 30. PMID: 21886862; PMCID: PMC3156403.

Dunn, A.M., 2009. Parasites and biological invasions. Adv. Parasitol. 68, 161–184.

Dunn, J.C., McClymont, H.E., Christmas, M., Dunn, A.M., 2009. Competition and parasitism in the native White Clawed Crayfish *Austropotamobius pallipes* and the invasive Signal Crayfish *Pacifastacus leniusculus* in the UK. Biol. Invasions 11, 315–324.

Dunn, A.M., Hatcher, M.J., 2015. Parasites and biological invasions: Parallels, interactions, and control. Trends Parasitol. 31 (5), 189–199.

Dunn, A.M., Blakeslee, A.M., Bojko, J., 2023. Parasites in Biological Invasions: an Introduction. In: Parasites and Biological Invasions. CABI, GB, pp. 1–7.

Everard, M., Gray, J., Wilkins-Kindemba, V., Cowx, I.G., 2009. Impacts of invasive species on ecosystem services: The case of the signal crayfish (*Pacifastacus leniusculus*). Environ. Law Manage. 21 (5), 250.

Foster, R., Peeler, E., Bojko, J., Clark, P.F., Morritt, D., Roy, H.E., Stebbing, P., Tidbury, H.J., Wood, L.E., Bass, D., 2021. Pathogens co-transported with invasive non-native aquatic species: Implications for risk analysis and legislation. NeoBiota 69, 79–102. https://doi.org/10.3897/neobiota.71358.

Grandjean, F., Gilbert, C., Razafimafondy, F., Vucić, M., Delaunay, C., Gindre, P., Moumen, B., 2019. A new bunya-like virus associated with mass mortality of white-clawed crayfish in the wild. Virology 533, 115–124.

Gabaldón, T., Völcker, E., Torruella, G., 2022. On the biology, diversity and evolution of nucleariid amoebae (Amorphea, Obazoa, Opisthokonta). Protist 173 (4), 125895.

Hatcher, M.J., Dick, J.T., Bojko, J., Stentiford, G.D., Stebbing, P., Dunn, A.M., 2019. Infection and invasion: Study cases from aquatic communities. In: Wilson, K., Fenton, A., Tompkins, D. (Eds.), Wildlife Disease Ecology. Cambridge University Press, pp. 262–295.

Hodson, J., South, J., Cancellario, T., Guareschi, S., 2024. Multi-method distribution modelling of an invasive crayfish (*Pontastacus leptodactylus*) at Eurasian scale. Hydrobiologia.

Ion, M.C., et al., 2024. World of Crayfish™: A web platform towards real-time global mapping of freshwater crayfish and their pathogens. PeerJ 12, e18229.

Jiang, J., Erickson, A., Qiao, W., Matsumura, E.E., Falk, B.W., 2023. Flock house virus as a vehicle for aphid Virus-induced gene silencing and a model for aphid biocontrol approaches. J. Pest. Sci. 96 (1), 225–239.

Jones, P., Binns, D., Chang, H.Y., Fraser, M., Li, W., McAnulla, C., Hunter, S., 2014. InterProScan 5: Genome-scale protein function classification. Bioinformatics 30 (9), 1236–1240.

Keane, R.M., Crawley, M.J., 2002. Exotic plant invasions and the enemy release hypothesis, Trends Ecol. Evolut., 17(4), 2002, 164–170. ISSN 0169-5347, https://doi.org/10.1016/S0169-5347(02)02499-0.

Kuzucu, O., yÖzcan, M., 2025. Caracterización molecular e identificación de Shewanella putrefaciens y aislamiento y caracterización morfológica de su fagolítico. Revista Científica De La Facultad De Ciencias Veterinarias 35 (1), 7. https://doi.org/10.52973/rcfcv-e35537.

Longshaw, M., Bateman, K.S., Stebbing, P., Stentiford, G.D., Hockley, F.A., 2012. Disease risks associated with the importation and release of non-native crayfish species into mainland Britain. Aquat. Biol. 16, 1–15. https://doi.org/10.3354/ab00417.

Mergaert, J., Cnockaert, M.C., Swings, J., 2003. *Thermomonas fusca* sp. nov. and Thermomonas brevis sp. nov., two mesophilic species isolated from a denitrification reactor with poly(E-caprolactone) plastic granules as fixed bed, and emended description of the genus Thermomonas. Int. J. Syst. Evol. Microbiol. 53, 1961–1966.

Miura, O., Torchin, M.E., 2023. Parasite release and biological invasions. In: Parasites and Biological Invasions. CABI, GB, pp. 24–41.

Nguyen, L.T., Schmidt, H.A., Von Haeseler, A., Minh, B.Q., 2015. IQ-TREE: a fast and effective stochastic algorithm for estimating maximum-likelihood phylogenies. Mol. Biol. Evol. 32 (1), 268–274.

Otto, M., 2012. (2012) Molecular basis of Staphylococcus epidermidis infections. Semin. Immunopathol. 34, 201–214. https://doi.org/10.1007/s00281-011-0296-2.

Peay, S., Holdich, D.M., Brickland, J., 2010. Risk assessments of non-indigenous crayfish in Great Britain. Freshwater Crayfish 17 (1), 109–122.

Petersen, J.M., Burgess, A.L., van Oers, M.M., Herniou, E.A., Bojko, J. (2024) Nudiviruses in free-living and parasitic arthropods: evolutionary taxonomy, Trends in Parasitology, 744, 762, 40, 8, Elsevier, 1471-4922.

Quaglio, F., Morolli, C., Galuppi, R., Tampieri, M.P., Marcer, F., Rotundo, G., 2004. Pathological investigation on crayfish (*Procambarus clarkii*, Girard 1852) from canals in Padana Plain. David Rogers Associates, DERBY.

Rainey, P.B., 1999. Adaptation of Pseudomonas fluorescens to the plant rhizosphere. Environ. Microbiol. 1, 243–257.

Reisinger, L.S., Petersen, I., Hing, J.S., Davila, R.L., Lodge, D.M., 2015. Infection with a trematode parasite differentially alters competitive interactions and antipredator behaviour in native and invasive crayfish. Freshw. Biol. 60 (8), 1581–1595.

Remnant, E.J., Baty, J.W., Bulgarella, M., Dobelmann, J., Quinn, O., Gruber, M.A.M., Lester, P.J., 2021. A diverse viral community from predatory wasps in their native and invaded range, with a new virus infectious to honey bees. Viruses 13, 1431. https://doi.org/10.3390/v13081431.

Rosewarne, P.J., Mortimer, R.J.G., Dunn, A.M., 2012. Branchiobdellidan infestation on endangered white-clawed crayfish (*Austropotamobius pallipes*) in the UK. Parasitology 139 (6), 774–780.

Salighehzadeh, R., Sharifiyazdi, H., Akhlaghi, M., Khalafian, M., Gholamhosseini, A., Soltanian, S., 2019. Molecular and clinical evidence of *Aeromonas hydrophila* and *Fusarium solani* co-infection in narrow-clawed crayfish *Astacus leptodactylus*. Dis Aquat Org 132, 135–141. https://doi.org/10.3354/dao03309.

Schwebke, J.R., Muzny, C.A., Josey, W.E., 2014. Role of gardnerella vaginalis in the pathogenesis of bacterial vaginosis: A conceptual model. J Infect Dis 210 (3), 338–343. https://doi.org/10.1093/infdis/jiu089.

Stratton, C.E., DiStefano, R., 2021. Is native crayfish conservation a priority for United States and Canadian fish and wildlife agencies? Freshwater Crayfish. 26, 25–36. https://doi.org/10.5869/fc.2021.v26-1.25.

Stratton, C.E., Moler, P., Allain, T.W., Reisinger, L.S., Behringer, D.C., Bojko, J., 2022a. The plot thickens: *Ovipleistophora diplostomuri* infects two additional species of Florida crayfish. J. Invertebr. Pathol. 191, 107766.

Stratton, C.E., Reisinger, L.S., Behringer, D.C., Bojko, J., 2022b. Revising the freshwater *Thelohania* to *Astathelohania* gen. et comb. nov., and description of two new species. Microorganisms 10 (3), 636.

Stratton, C.E., Reisinger, L.S., Behringer, D.C., Reinke, A.W., Bojko, J., 2023a. *Alternosema astaquatica* n. sp.(Microsporidia: Enterocytozoonida), a systemic parasite of the crayfish Faxonius virilis. J. Invertebr. Pathol. 199, 107948.

Stratton, C.E., Kabalan, B.A., Bolds, S.A., Reisinger, L.S., Behringer, D.C., Bojko, J., 2023b. Cambaraspora faxoni n. sp.(Microsporidia: Glugeida) from native and invasive crayfish in the USA and a novel host of Cambaraspora floridanus. J. Invertebr. Pathol. 199, 107949.

Stratton, C.E., Bolds, S.A., Reisinger, L.S., Behringer, D.C., Khalaf, A., Bojko, J., 2024a. Microsporidia and invertebrate hosts: genome-informed taxonomy surrounding a new lineage of crayfish-infecting *Nosema* spp. (Nosematida). Fungal Divers. 128 (1), 167–190.

Stratton, C.E., Reisinger, L.S., Behringer, D.C., Gray, S.N., Larson, E.R., Bojko, J., 2024b. North American crayfish harbour diverse members of the Nudiviridae. Virology 598, 110183.

Sun, M., Li, T., Liu, Y., Wilson, K., Chen, X., Graha, R.I., Yang, X., Ren, G., Xu, P., 2024. A dicistrovirus increases pupal mortality in Spodoptera frugiperda by suppressing protease activity and inhibiting larval diet consumption. J. Integr. Agric. 23 (8), 2723–2734. https://doi.org/10.1016/j.jia.2023.12.030.

Svoboda, J., Mrugała, A., Kozubíková-Balcarová, E., Petrusek, A., 2017. Hosts and transmission of the crayfish plague pathogen *Aphanomyces astaci*: A review. J. Fish Dis. 40 (1), 127–140.

Taştan, B., Akhan, S., 2021. Molecular identification of burn spot disease syndrome agent Fusarium avenaceum in Turkish crayfish Pontastacus leptodactylus populations. Dis. Aquat. Org. 144, 33–40. https://doi.org/10.3354/dao03570.

Triplett, L.R., Verdier, V., Van Malderghem, T.C., Cleenwerck, I., Maes, M., Deblais, L., Corral, R., Koita, O., Cottyn, B., Leach, J.E., 2015. Characterization of a novel clade of Xanthomonas isolated from rice leaves in Mali and proposal of Xanthomonas maliensis sp. nov. Antonie Van Leeuwenhoek. 107 (4), 869–881. https://doi.org/10.1007/s10482-015-0379-5. Epub 2015 Jan 15. PMID: 25588569.

Weon, H.Y., Kim, B.Y., Kwon, S.W., Park, I.C., Cha, I.B., Tindall, B.J., Stackebrandt, E., Trüper, H.G., Go, S.J., 2005. Leadbetterella byssophila gen. nov., sp. nov., isolated from cotton-waste composts for the cultivation of oyster mushroom. Int J Syst Evol Microbiol. 55 (Pt 6), 2297–2302. https://doi.org/10.1099/ijs.0.63741-0. PMID: 16280486.

Williamson, M., 1996. Biological Invasions, Population and Community Biology Series, ISSN 1367-5257. Springer Science & Business Media, Netherlands.

Wood, L.E., Clinton, M., Bass, D., Bojko, J., Foster, R., Guilder, J., Tidbury, H., 2023. Parasite invasions and food security. In: Parasites and Biological Invasions. CABI, GB, pp. 141–158.

Zhang, D.C., Schumann, P., Liu, H.C., Xin, Y.H., Zhou, Y.G., Schinner, F., Margesin, R., 2010. Arthrobacter alpinus sp. nov., a psychrophilic bacterium isolated from alpine soil. Int. J. Syst. Evol. Microbiol. 60, 2149–2153.

Zimmermann, L., Stephens, A., Nam, S.Z., Rau, D., Kübler, J., Lozajic, M., Alva, V., 2018. A completely reimplemented MPI bioinformatics toolkit with a new HHpred server at its core. J. Mol. Biol. 430 (15), 2237–2243.